Vol 17 No 6, June 2008
1674-1056/2008/17(06)/2160-10

Chinese Physics B

© 2008 Chin. Phys. Soc.
and IOP Publishing Ltd

Slowly moving matter–wave gap soliton propagation in weak random nonlinear potential*

Zhang Ming-Rui(张铭锐)[a)b)†], Zhang Yong-Liang(张永亮)[b)],
Jiang Xun-Ya(蒋寻涯)[b)], and Zi Jian(资 剑)[a)]

[a)] *Surface Physics Laboratory (National Key Lab), Fudan University, Shanghai* 200433, *China*

[b)] *Institute of Microsystem and Information Technology, Chinese Academy of Sciences, Shanghai* 200050, *China*

(Received 15 May 2007; revised manuscript received 25 December 2007)

We systematically investigate the motion of slowly moving matter–wave gap solitons in a nonlinear potential, produced by the weak random spatial variation of the atomic scattering length. With the weak randomness, we construct an effective-particle theory to study the motion of gap solitons. Based on the effective-particle theory, the effect of the randomness on gap solitons is obtained, and the motion of gap solitons is finally solved. Moreover, the analytic results for the general behaviours of gap soliton motion, such as the ensemble-average speed and the reflection probability depending on the weak randomness are obtained. We find that with the increase of the random strength the ensemble-average speed of gap solitons decreases slowly where the reduction is proportional to the variance of the weak randomness, and the reflection probability becomes larger. The theoretical results are in good agreement with the numerical simulations based on the Gross–Pitaevskii equation.

Keywords: gap soliton, weak random nonlinear potentials, effective particle picture
PACC: 4265S

1. Introduction

In the past years, Bose–Einstein condensates (BECs) in optical lattices have aroused much theoretical and experimental interest.[1,2] They provide a wealth of fascinating physical phenomena covering Bloch oscillation,[3] Landau–Zener tunnelling,[4] lensing effect[5] and quantum phase transition of the Mott insulator type.[6] In the mean-field approximation these systems can be treated as nonlinear periodic systems, where the periodic potential results from the interference of laser beams and the nonlinearity comes from the two-body interatomic interactions appropriate for dilute Bose gases. In such nonlinear periodic systems, an important phenomenon is the formation of the gap soliton (GS).[7] The term 'gap soliton' was first proposed by Chen and Mills when they studied light propagation in periodic Kerr materials.[8] In optics, when the material refraction index exhibits periodicity on the scale of light wavelength, a photonic band gap is formed, and an optical pulse with frequencies in the frequency gap cannot propagate in such a material. Chen and Mills showed that the nonlinearity could lead the optical pulse to be localized when the frequencies lie in the gap, and the localized wave packets are called GSs. Since then, GSs have been intensively studied in optical systems and BEC systems.[7,9−22] Many theoretical methods such as the coupled-mode theory[9,12,13,22] and the multi-scale expansion method[11] have been developed to describe the evolutions of GSs. All the studies reveal that GSs are the solitary waves inside the nonlinear periodic systems. Recently, a matter wave GS is directly observed experimentally in a ^{87}Rb BEC containing about 250 atoms.[7]

Among these studies, GS propagation in a nonuniform medium is another interesting subject. In optical systems, GS propagation in nonuniform lattices where the lattice constants changed continuously had been studied by Broderick and Sterke.[23] In their study, the slow change of lattice constants was treated as a perturbation and the motion of GS was described by an effective particle picture (EPP). In the EPP, the GS can be treated as a particle with effective forces acting on it. But so far, matter wave GS propagation, when the mean-field nonlinearity is weakly random in space, has not been studied yet.

In this paper, we investigate that slowly moving

*Project supported by the National Basic Research Program of China (Grant No 2006CB921701-6), Pujiang Talent Project (Grant No PJ2005(00593)), and the Hundred Tarent Project of the Chinese Academy of Sciences, China.
†E-mail: mrzhang@mail.sim.ac.cn

matter–wave GSs propagate in a weak random nonlinear potential, produced by the weak random variations of atomic scattering lengths in space. The strength of interatomic interaction, i.e. the value of the atomic scattering length a_s, can be varied by using the Feshbach resonance (FR) method.[24,25] For example, if the one-dimensional BEC is close to the magnetic wire, then the spatially random magnetic field fluctuation can be induced by any small variation of current. In this paper, we focus our attention on matter wave GSs in a shallow optical lattice. Therefore, GSs can be described by the coupled-mode theory. Based on the previous studies,[23,26] an effective-particle theory is introduced into the weak nonlinear random system. According to the effective-particle theory, the effects of the weak randomness on GSs are obtained. We find that with the weak randomness a conservative 'force' is generated to change the GS local velocity, and that the GS propagates in a conservative potential just as a classical particle propagates in that potential. The detailed expressions of the effective forces and potentials are obtained. The effective force can be divided into two parts, i.e. the GS front part and the back part, and the 'force-responding' effects of the weak randomness on two parts are different. And the effective potential strongly depends on the local configuration of the randomness. With the effective potential, the GS motion can be predicted exactly. Moreover, the general behaviours of GS motion depending on the randomness are obtained. With the increase of the random strength, the ensemble-average speed decreases slowly and its reduction is proportional to the variance of the randomness. And the reflection probability becomes larger along with the random strength. To confirm the theoretical results obtained by the EPP, we also simulate the time evolutions of matter–wave GSs using the finite-difference time-domain (FDTD) method based on the Gross–Pitaevskii equation (GPE).[27] All the results obtained from the EPP are consistent with the results from the numerical simulations based on the GPE.

The remainder of the present paper is organized as follows. In Section 2, we introduce the setup of the system in detail. In Section 3, the EPP based on the coupled-mode theory is constructed. And the detailed expressions of the effective force and the effective potential are derived. In Section 4, using the EPP and the numerical FDTD method, the trajectories of GSs are obtained. And a general behaviour of the ensemble-average speed depending on the weak randomness is obtained. Finally, in Section 5, we summarize our results from the present study.

2. The setup of the system

In the mean-field approximation, the dynamic evolution of a nonlinear matter–wave in one-dimensional optical lattices can be described by the dimensionless GPE[28]

$$\mathrm{i}\frac{\partial u}{\partial t} = -\frac{1}{2}\frac{\partial^2 u}{\partial x^2} + V\sin^2\left(\frac{x}{2}\right)u + c(x)|u|^2 u, \qquad (1)$$

where u is the wave function, with $\int |u|^2 \mathrm{d}x = N$, N is the number of atoms; V is the depth of the optical lattices; $c(x)$ is the spatially dependent dimensionless mean-field nonlinear coefficient which results from the weak randomness of the atomic scattering length. In this paper we assume the nonlinear coefficients in different optical lattice cells to be different. Then the nonlinear coefficient can be written as

$$c(x_i) = c_0(1 + W\gamma_i)\ , \qquad (2)$$

in which c_0 is the average mean-field nonlinear coefficient, $W \ll 1$ is the strength of the weak randomness and γ_i is the random number to characterize the randomness. In the system, the random numbers are assumed to satisfy the Gaussian distribution

$$\rho(\gamma) = C_\gamma \mathrm{e}^{-\gamma^2/\sigma_\gamma^2}\ , \qquad (3)$$

where $\sigma_\gamma = 1$ is the root mean square value of Gaussian distribution, and $C_\gamma = \dfrac{1}{\sqrt{\pi}}$ is the normalized coefficient.

To study the motion of GSs in a weak nonlinear random system, the setup of the system is shown in Fig.1. In region I ($x < 0$), the randomness of the interatomic interaction is absent, (i.e. $c(x) = c_0$), and a moving GS with the initial velocity v_0 is generated and then enters into region II. In region II ($x > 0$), the weak spatial variations of the atomic scattering length are considered, this means that the spatial variations of the nonlinear coefficients are random in space. We will study the GS motion theoretically and numerically. Theoretically, the EPP is constructed to describe GS propagation in weak random nonlinear potentials. Numerically, the GS motion is simulated by the FDTD method. In addition, the general behaviours of GS motion, i.e. the ensemble-average speed and the reflection, are also obtained.

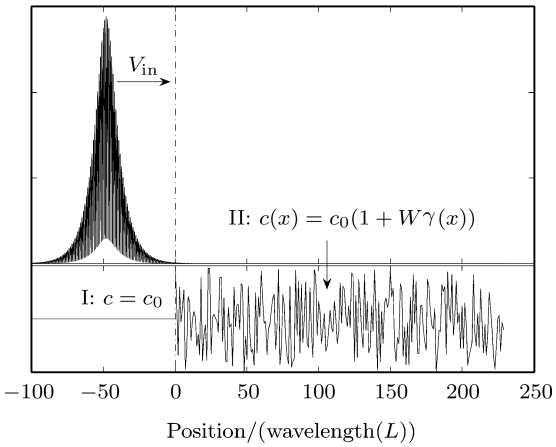


Fig.1. A GS with initial speed $v_{\rm in}$ moving from region I without the randomness, and then propagating in region II where the weak random nonlinear potential is considered.

3. Effective particle picture

In this section, the EPP description based on the coupled-mode theory is constructed and the effect of the weak nonlinear randomness on GS is obtained.

Matter wave GSs in shallow optical lattices have been studied by the coupled-mode theory extensively.[22] According to the coupled-mode description, the wave function u can be expanded as a forward wave and a backward wave as follows:

$$u(x,t) = [u_{\rm f}(x,t)\mathrm{e}^{\mathrm{i}k_{\rm L}x} + u_{\rm b}(x,t)\mathrm{e}^{-\mathrm{i}k_{\rm L}x}]\mathrm{e}^{-\mathrm{i}\mu t}, \quad (4)$$

where μ is the chemical potential of the matter wave, $k_{\rm L} = 0.5$ is the dimensionless laser wave vector, and the slowly varying variables $u_{\rm f}$ and $u_{\rm b}$ are the amplitudes of the fields propagating forwards and backwards, respectively. Substituting expression (4) into Eq.(1), we can obtain the nonlinear coupled-mode equations (NLCMEs):

$$\mathrm{i}\frac{\partial u_{\rm f}}{\partial x} + \frac{\mathrm{i}}{k_{\rm L}}\frac{\partial u_{\rm f}}{\partial t} + \Delta k u_{\rm f} + \kappa u_{\rm b} + \alpha(x)(|u_{\rm f}|^2 + 2|u_{\rm b}|^2)u_{\rm f} = 0\ , \quad (5)$$

and

$$-\mathrm{i}\frac{\partial u_{\rm b}}{\partial x} + \frac{\mathrm{i}}{k_{\rm L}}\frac{\partial u_{\rm b}}{\partial t} + \Delta k u_{\rm b} + \kappa u_{\rm f} + \alpha(x)(2|u_{\rm f}|^2 + |u_{\rm b}|^2)u_{\rm b} = 0\ , \quad (6)$$

where $\Delta k = (2\mu - k_{\rm L}^2 - V/2)/2k_{\rm L}$ is the value to represent the difference between the chemical potential and the gap centre, $\kappa = V/4k_{\rm L}$ is the coupling coefficient, and $\alpha(x) = -c_0(1 + W\cdot\gamma)/k_{\rm L}$ is the nonlinear coefficient, from which the weak nonlinear randomness is introduced into the coupled-mode theory.

In region I, in which the nonlinear randomness is absent, the strict moving GS solutions supported by the NLCMEs (5) and (6) can be written as[12,13]

$$u_{\rm f,b}(x,t) = A_{\rm f,b}(x,t)\mathrm{e}^{\mathrm{i}\phi_{\rm f,b}}\ , \quad (7)$$

where

$$A_{\rm f} = \left(\frac{\kappa}{\alpha_0}\frac{2(1+\beta)\sqrt{1-\beta^2}}{3-\beta^2}\frac{\cos^2\theta}{\sin(\theta)+\cosh[2y]}\right)^{1/2}\ , \quad (8)$$

$$A_{\rm b} = \left(\frac{\kappa}{\alpha_0}\frac{2(1-\beta)\sqrt{1-\beta^2}}{3-\beta^2}\frac{\cos^2\theta}{\sin(\theta)+\cosh[2y]}\right)^{1/2}\ , \quad (9)$$

$$\phi_{\rm f} = \phi_0 + \left(\frac{4\beta}{3-\beta^2}+1\right)\arctan\left(\frac{\cos\theta}{1+\sin\theta}\tanh[y]\right) + (\beta\tan\theta)\,y - \frac{\pi}{2}\ , \quad (10)$$

and

$$\phi_b = \phi_0 + \left(\frac{4\beta}{3-\beta^2}-1\right)\arctan\left(\frac{\cos\theta}{1+\sin\theta}\tanh[y]\right) + (\beta\tan\theta)y + \frac{\pi}{2} \quad (11)$$

where $\beta = v/k_{\rm L}$ is the GS normalized speed and v is the GS speed, $\theta = \arcsin\dfrac{\Delta k}{\kappa_0\sqrt{1-\beta^2}}$ and $y = \dfrac{\kappa_0\cos\theta}{\sqrt{1-\beta^2}}(x - x_{\rm c} - vt)$ are the moving coordinates in which $x_{\rm c}$ is the GS central position. The spatial distribution of a moving GS solution is plotted in Fig.2. From this figure, we can see that it is laterally symmetric in space.

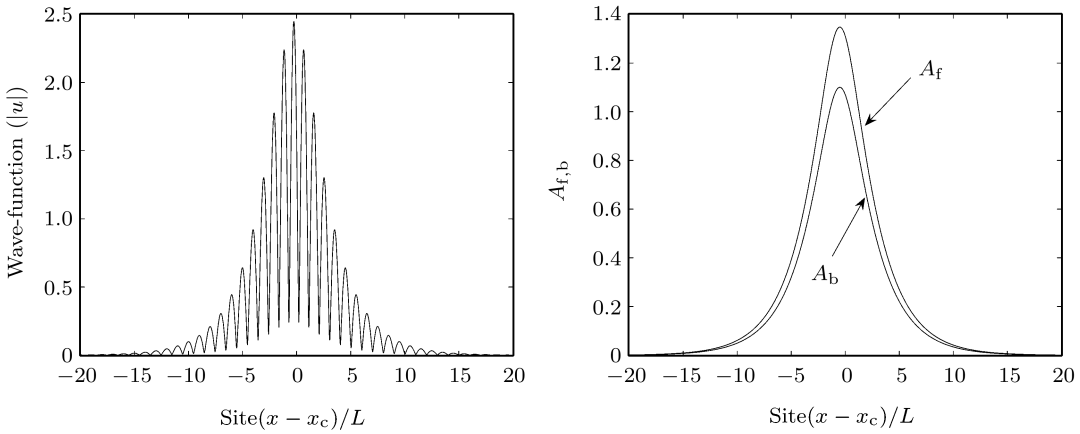


Fig.2. Solutions of moving GS in the system without weak randomness with parameters: chemical potential $\mu = 0.129$, optical potential $V_0 = 0.04$, nonlinear coefficient $c_0 = -0.01$, and the speed $v_{in} = 0.10$, showing that the spatial distribution of GS is laterally symmetric in space.

In region II, the spatial randomness of the nonlinearity is considered, and the exact GS solutions do not exist. However, because the nonlinear randomness is so weak that it can be treated as a perturbation, we can make the assumption of EPP. Under the assumption, the matter wave field can be always treated as a GS. This is true as long as the radiation of GS fields can be negligible. Under this assumption, the strict GS solution is assumed to be still available in region II. From the GS solutions in expression (7), we can see that the time evolutions of parameters θ and β fully characterize the GS. Therefore, the aim of the EPP is to find the evolution equations of θ and β. Similar to the study in Refs.[23, 26], the EPP can be derived by defining a small set of variables which can completely characterize the GS motion in the absence of spatial randomness. The variables are defined as follows:
the total particle number

$$Q \equiv \int_{-\infty}^{+\infty} (|u_f|^2 + |u_b|^2) \mathrm{d}x \ , \tag{12}$$

the effective position

$$x_{\text{eff}} \equiv \frac{1}{Q} \int_{-\infty}^{+\infty} x(|u_f|^2 + |u_b|^2) \mathrm{d}x, \tag{13}$$

the effective speed

$$v_{\text{eff}} \equiv \frac{1}{Q} \int_{-\infty}^{+\infty} (|u_f|^2 - |u_b|^2) \mathrm{d}x, \tag{14}$$

and the effective momentum

$$P \equiv \int_{-\infty}^{+\infty} \mathrm{Im}[u_f^* \partial_x u_f + u_b^* \partial_x u_b] \mathrm{d}x. \tag{15}$$

For strict GS solutions, the values of the above variables are as follows: $Q = \frac{4}{\alpha_0} \frac{1-\beta^2}{3-\beta^2} (\frac{\pi}{2} - \theta)$, $x_{\text{eff}} = x_c + vt$, $v_{\text{eff}} = v$ and $P = \frac{\kappa}{\alpha_0} \frac{4\beta\sqrt{1-\beta^2}}{3-\beta^2} \cos\theta + \frac{\kappa}{\alpha_0} \frac{16\beta\sqrt{1-\beta^2}}{(3-\beta^2)^2} \left[\cos\theta - \sin\theta \left(\frac{\pi}{2} - \theta\right)\right]$. In these variables, the particle number Q and the momentum P are both conserved quantities without randomness.

With the weak nonlinear randomness, using the definition of variables (12)–(15) and the NLCMEs, time derivatives of the total particle number (Q), effective momentum (P) and effective position (x_{eff}) can be easily calculated

$$\frac{\mathrm{d}Q}{\mathrm{d}t} = 0, \tag{16}$$

$$\begin{aligned} F &= \frac{\mathrm{d}P}{\mathrm{d}t} \\ &= \frac{1}{2}\alpha_0 W \int_{-\infty}^{+\infty} \left[|u_f|^4 + |u_b|^4 + 4|u_f^2||u_b^2| \frac{\partial \gamma}{\partial x} \right] \mathrm{d}x \\ &= -\frac{1}{2}\alpha_0 W \int_{-\infty}^{+\infty} \gamma \mathrm{d}x \frac{\partial[|u_f|^4 + |u_b|^4 + 4|u_f^2||u_b^2|]}{\partial x}, \end{aligned} \tag{17}$$

and

$$\frac{\mathrm{d}x_{\text{eff}}}{\mathrm{d}t} = \frac{1}{Q} \int_{-\infty}^{+\infty} (|u_f|^2 - |u_b|^2) \mathrm{d}x = v_{\text{eff}}. \tag{18}$$

Because the time derivatives of the above variables can be obtained from the definitions of the variables, Eq.(16) means that the particle number is conserved only if the amplitudes u_f and u_b obey the NLCMEs. Equation (17) represents the effect of the weak nonlinear randomness on GS. And Eq.(18) confirms that the definitions of position and speed given by expressions (13) and (14) are mutually consistent.

In Eq.(17), the force can be obtained by performing the integrals. To obtain the integrals, the field

$(u_{\rm f,b})$ must be known at all times, which means that the full NLCMEs should be solved first. Instead, as mentioned above, the moving GS is assumed to be the same as a strict GS solution except for the speed and related parameters. Furthermore, since $\mathrm{d}Q/\mathrm{d}t = 0$, the parameter $\theta(t)$ can be expressed in terms of the normalized speed $\beta(t)$ and the initial particle number Q_0 as

$$\theta(t) = \frac{\pi}{2} - \frac{\alpha}{4}\frac{3-\beta^2}{1-\beta^2}Q_0. \tag{19}$$

So the GS motion can be fully characterized by the evolution of normalized speed β.

In this paper, we focus attention only on the slowly moving case. From expression (19), we can see that the change of the parameter θ is just of the order of β^2. This means that the parameter θ can be treated as a speed-independent variable in the low speed limit ($\beta \ll 1$). And the momentum P in expression (15) can be approximated as

$$\begin{aligned} P &= \frac{\kappa_0}{\alpha_0}\left[\frac{4}{3}\cos\theta + \frac{16}{9}\left(\cos\theta - \sin\theta\left(\frac{\pi}{2}-\theta\right)\right)\right]v \\ &= m_{\rm s}\beta\ . \end{aligned} \tag{20}$$

In Expression (20), the parameter $m_{\rm s}$ is also speed-independent, and it can be treated as the mass of GS. On the other hand, in the low-speed limit the change of function $\partial_x(|u_{\rm f}|^4 + |u_{\rm b}|^4 + 4|u_{\rm f}^2||u_{\rm b}^2|)$ is also just of the order of β^2, so the force in expression (17) can be seen as a conservative one, and we can introduce an effective potential later.

Based on the above analysis, in the low speed limit the equations to describe the GS motion in the EPP are listed as follows:

$$\frac{\mathrm{d}x_{\rm eff}}{\mathrm{d}t} = \beta k_{\rm L}, \tag{21}$$

$$F = \frac{\mathrm{d}P}{\mathrm{d}t}, \tag{22}$$

and

$$P = m_{\rm s}\beta\ . \tag{23}$$

To examine the GS motion, the force in expression (22) should be obtained first. After introducing the 'force-responding' function $g(x-x_{\rm c}) = -\frac{1}{2}\partial_x(|u_{\rm f}|^4 + |u_{\rm b}|^4 + 4|u_{\rm f}^2||u_{\rm b}^2|)$,[29] the force can be simply written as

$$F(x_{\rm c}) = \alpha_0 W\int_{-\infty}^{+\infty} g(x)\gamma(x)\mathrm{d}x. \tag{24}$$

The spatial distribution of the 'force-responding' function is plotted in Fig.3. From this figure, we can see that the force-responding function $g(x-x_{\rm c})$ is odd: $g(x_{\rm c}+x) = -g(x_{\rm c}-x)$ (the odd property can also be obtained from the GS solution), and when $|x-x_{\rm c}| \to \infty$, then $g(x) \to 0$. To simplify the calculation, we introduce a cutoff length, $x_{\rm cut}$, and suppose that when $|x-x_{\rm c}| > x_{\rm cut}$, then $g(x) \approx 0$. Now the force in expression (24) can be approximated as

$$\begin{aligned} F(x_{\rm c}) \approx\ & \alpha_0 W\int_0^{x_{\rm cut}} g(x_{\rm c}+x)\gamma(x_{\rm c}+x)\mathrm{d}x \\ & +\alpha_0 W\int_{-x_{\rm cut}}^{0} g(x_{\rm c}+x)\gamma(x_{\rm c}+x)\mathrm{d}x \\ =\ & F_{\rm f}(x_{\rm c}) + F_{\rm b}(x_{\rm c}). \end{aligned} \tag{25}$$

Because the force-responding function $g(x-x_{\rm c})$ is odd, the force effects of the randomness on the GS front part and its back part are different. For instance, when $\gamma(x) > 0$, if the position x is in GS front part then its contribution to the total force is positive (forward force), but if the position x is in its back part, then its contribution is negative (backward force). In other words, the total force in expression (25) can be divided into two parts: $F_{\rm f}(x_{\rm c}) = \kappa_0 W\int_0^{x_{\rm cut}} g(x_{\rm c}+x)\gamma(x_{\rm c}+x)\mathrm{d}x$, which is the 'front-part' and it is the integral of all contributions of the local fluctuation in the region of the GS front part, and $F_{\rm b}(x_{\rm c}) = \kappa_0 W\int_{-x_{\rm cut}}^{0} g(x_{\rm c}+x)\gamma(x_{\rm c}+x)\mathrm{d}x$, which is the 'back-part'. Expression (25) gives a detailed interpretation to the origin of the force from the odd property of the force-responding function.

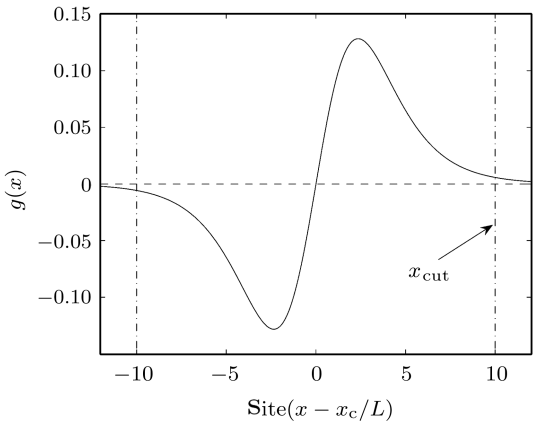


Fig.3. The spatial distribution of force-responding function $g(x)$. The parameters of GS are the same as those in Fig.2. We can see that the force-responding function is odd, and when $|x-x_{\rm c}| > n_{\rm cut}L$, $g(x)$ is so small that it is negligible.

Since the force F depends only on the configu-

ration in which the GS is, an effective potential can be defined to describe the GS motion. The potential $U(x_c)$ at position x_c is defined as

$$U(x_c) = -\int_{x_0}^{x_c} F(x')\mathrm{d}x' \ , \tag{26}$$

where x_0 is the initial position of GS. The force in expression (26) at position x' can be discretized as

$$F(x') = \sum_{i=n'-n_{\mathrm{cut}}}^{i=n'+n_{\mathrm{cut}}} \lambda_i \gamma_i, \tag{27}$$

where $n' = x'/L$ and the values of coefficient $\lambda_i = \alpha_0 W \int_{(i-1)L}^{iL} g(x-x')\mathrm{d}x$ satisfy $\sum_i \lambda_i = 0$. Substituting expression (27) into expression (26), the effective potential U at position x_c can be finally given by

$$\begin{aligned} & U(x_c) \\ &= -\alpha_0 LW \left[\sum_{j=1}^{n_{\mathrm{cut}}} (\gamma_{n_c-j} + \gamma_{n_c+j}) \int_{jL}^{n_{\mathrm{cut}}L} \mathrm{d}t g(x_c+t) \right. \\ &\quad \left. - \sum_{j=1}^{n_{\mathrm{cut}}} (\gamma_{n_0-j} + \gamma_{n_0+j}) \int_{jL}^{n_{\mathrm{cut}}L} \mathrm{d}t g(x_0+t) \right], \end{aligned} \tag{28}$$

where $n_c = x_c/L$, $n_{\mathrm{cut}} = x_{\mathrm{cut}}/L$, and $n_0 = x_0/L$. Since GS starts from the position without randomness (i.e. $\gamma_{n_0+j} = 0$, and $|j| < n_{\mathrm{cut}}$), the second term in expression (28) is zero. To express the potential in expression (28) more concisely, we introduce a weight function as

$$R(\gamma_{n_c \pm j}) = -\int_{jL}^{n_{\mathrm{cut}}L} \mathrm{d}t g(x_c + x). \tag{29}$$

And the effective potential can be written as

$$U(x_c) = \alpha_0 LW \sum_{j=-n_{\mathrm{cut}}}^{n_{\mathrm{cut}}} R(\gamma_{n_c+j}) \gamma_{n_c+j}. \tag{30}$$

Obviously, the weight function depends only on the GS fields u_{f} and u_{b}, then it can be treated as the contribution of local randomness to the effective potential. The spatial distribution of the weight function $R(\gamma_{n_c+j})$ normalized by $R(\gamma_{n_c})$ is plotted in Fig.4. From this figure, we can see that the weight function is even (the even property can be also obtained from expression (29)). This is because the function depends only on the field distribution of GS which is laterally symmetric in space. Here we should point out that the force-responding function depends on the x-derivative of the field distribution which is odd in space. Finally, from expression (30), we can see that the potential strongly depends on the random configuration of the position where the GS is.

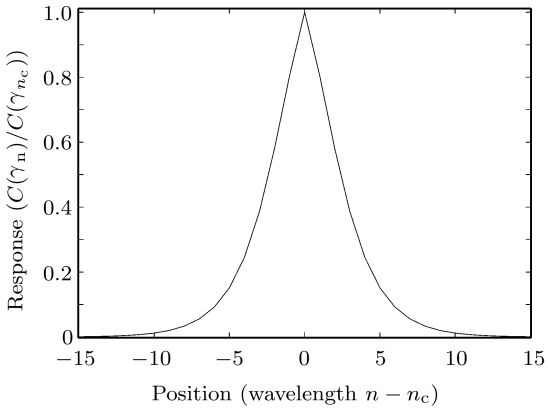


Fig.4. $C(\gamma_i)$ normalized by $C(\gamma_{i_c})$ versus position. The parameters of GS are the same as those in Fig.2. In this case $C(\gamma_{i_c}) = -3.52$. We can see that the response of the randomness to the effective potential mostly comes from the central sites of GS. And the contributions from the front part and the back part of GS are equal to each other.

Because the effective potential is conservative, the GS motion obeys the mechanical energy conservation

$$\frac{m_{\mathrm{s}}}{2}\beta^2(x) + U(x) = \frac{m_{\mathrm{s}}}{2}\beta^2(x_0) + U(x_0) \ , \tag{31}$$

where $\frac{1}{2}m_{\mathrm{s}}\beta^2$ is the 'kinetic energy' of GS in the EPP. Now we give a physical interpretation to the effective potential. If we combine the optical potential and the nonlinear potential into the lattice energy, the total energy should be conserved. In this sense, the effective potential can be treated as the lattice energy. For example, if the nonlinear coefficient becomes larger, the lattice energy becomes larger and the GS speed decreases. Furthermore, from expression (30), we can see that if $R_j < 0$ (because $c_0 < 0$ in this case the nonlinear coefficient c becomes larger), the potential becomes larger. In other words, the lattice energy is implicitly included in the effective potential. From this view, we give a clear physical meaning to the effective potential.

If the configuration of the randomness is known, the trajectories which describe the speed dependence on the position can be obtained. Since the GS starts from the position without randomness (region I), the potential $U(x_0)$ is zero. Then it follows from Eq.(31) that there exists a critical potential

$$U_{\mathrm{c}} = m_{\mathrm{s}}\beta_0^2/2 \ . \tag{32}$$

If all the potentials are smaller than the critical potential, the GS propagates forward. On the contrary, if the potentials are larger than the critical potential at some sites, GS will be reflected from these sites.

4. GS propagation in a weak random nonlinear potential

From the above analysis, we can see that the GS motion in a weak random nonlinear potential can be described by the EPP. On the other hand, the GS motion can be obtained from the direct numerical simulation based on the GPE. In this section, we will use the numerical simulation and the EPP assumption to study the GS motion in a weak nonlinear random potential.

In the numerical simulation, in order to avoid the reflection from the edges of the computational domain, absorbing boundary conditions in the form of perfectly matched layers (PMLs)[27] are assumed to hold on the edge of the numerical grids. The model Eq.(1) with PMLs is discretized via the Crank–Nicholson algorithm[27] and solved numerically with the finite difference time-domain (FDTD) method. In calculation 100 grid points per lattice site are used, which results in the grid spacing being much smaller than the length of the GS. To keep the numerical stability, the time grid is about $\delta t \sim 10^{-3}$. And the computational domain extends to over 500 lattice sites (about 25 times as large as the GS width).

In correspondence with the two kinds of motion mentioned in section 3, according to the FDTD method, we simulate the GS time evolutions for the propagation case and the reflection case separately. For the propagation case, the GS time evolution is shown in Fig.5(a). From this figure, we can see that the GS propagates forward. This accords with the analysis in Fig.5(b) which shows that the effective potential is always smaller than the critical potential. Moreover, we obtain the GS trajectories from the EPP and the numerical simulations. We can see that they are consistent with each other very well. For the reflection case, the GS evolution is plotted in Fig.6(a) which shows that the GS is reflected at time $t = 66\Delta t$. This coincides with the effective potential shown in Fig.6(b) which shows that in region III the effective potential is larger than the critical potential. Furthermore, the GS trajectories are plotted in Fig.6(c). Similar to the propagation case, two trajectories coincide with each other very well. The two examples confirm that the EPP is valid to describe the GS propagation in this weak nonlinear random system.

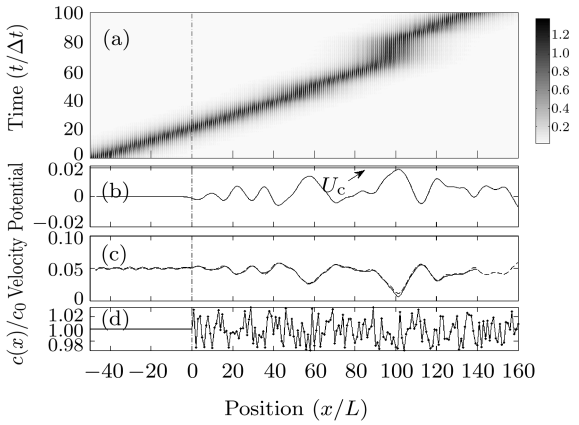


Fig.5. GS propagating through the weak random nonlinear potential, with parameters of GS being chemical potential $\mu = 0.129$, optical potential $V_0 = 0.04$, nonlinear coefficient $c = -0.01$, the initial speed $v_{\rm in} = 0.05$, and the random strength of the nonlinear potential $W = 0.035$. Panel (a) shows the evolution of GS calculated by the numerical simulation based on Eq.(1). Panel (b) exhibits the effective potential versus position. During the propagation, the effective potential is always smaller than the critical potential $U_{\rm c}$. Panel (c) displays the trajectories which are in the $(v-x)$ plane. The solid line shows the results obtained from the EPP approach, and the dash line represents the results from the exact numerical simulations. Panel (d) indicates the weak random configuration in space.

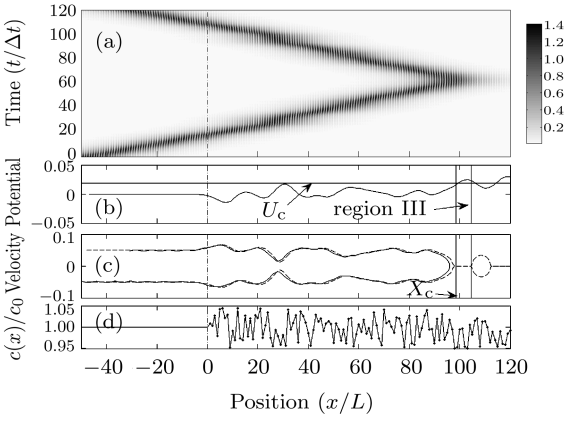


Fig.6. GS reflected from the weak random nonlinear potential. The parameters of GS are the same as those in Fig.5, and the random strength of the randomness is $W = 0.05$. Panel (a) shows time evolution of GS from the numerical simulation based on the GPE. Panel (b) displays the effective potential versus position x. We can see that in region III, the effective potential is larger than the critical value $U_{\rm c}$, and the GS is reflected. Panel (c) exhibits the trajectories that are in the $(v-x)$ plane. The solid line shows the results obtained from the EPP approach, and the dash line indicates the results from the exact numerical simulation. Panel (d) displays the weak random configuration in space.

From the above analysis, we can see that the local

speed is strongly dependent on the local random configuration. Next, we will obtain a general behaviour of the motion of GS dependent on the randomness. Generally, the GS motion is characterized by the normalized ensemble-average speed ($\overline{\beta}$), and the weak randomness is characterized by the random strength (W). The ensemble-average speed is defined as

$$\overline{\beta} = \frac{1}{k_{\mathrm{L}}} \lim_{N\to\infty} \frac{NL}{\sum_i \Delta t_i}, \tag{33}$$

where

$$\Delta t_i = \frac{L}{\beta_i k_{\mathrm{L}}} = \frac{L}{k_{\mathrm{L}}} \frac{1}{\sqrt{\beta_0^2 - \frac{2}{m_{\mathrm{s}}} U_i}} \tag{34}$$

is the time in which the GS passes through the ith cell.

In expression (34), the random potential can be written as $U_i = C_u W \gamma_u^i$, where W is the random strength, C_u is the coefficient, and γ_u^i is the random number to characterize the form of the random potential. Substituting expression (34) into expression (33) and transforming the discrete expression (33) into the integral form, the ensemble-average speed can be written as[30]

$$\overline{\beta} = \frac{1}{\int \mathrm{d}\gamma_u \frac{1}{\sqrt{1-\frac{2C_u W \gamma_u}{m_{\mathrm{s}}\beta_0^2}}} \cdot \rho(\gamma_u)}, \tag{35}$$

where $\rho(\gamma_u)$ is the distribution of the random number γ_u. In expression (35), if the coefficient C_u and the distribution function $\rho(\gamma_u)$ are obtained, the average speed can be easily obtained. From expression (28), the coefficient C_u and the random number γ_u are given respectively by

$$C_u = \alpha_0 g_0 L, \tag{36}$$

and

$$\gamma_u^{n_{\mathrm{c}}} = \sum_{j=-n_{\mathrm{cut}}}^{j=n_{\mathrm{cut}}} \eta_j \gamma_{n_{\mathrm{eff}}+j}, \tag{37}$$

where $g_0 = 2\sum_j [\int_{jL}^{n_{\mathrm{cut}}L} \mathrm{d}x g(x_{\mathrm{c}}+x)]$ and $\eta_i = R(\gamma_{n_{\mathrm{c}}+\mathrm{i}})/g_0$. Then the distribution of γ_u can be obtained as

$$\rho(\gamma_u) = C_{\gamma_u} \mathrm{e}^{-\gamma_u^2/\sigma_{\gamma_u}^2}, \tag{38}$$

where $\sigma_{\gamma_u} = 1 \Big/ \sqrt{\left[\sum_i \eta_i^2\right]}$ is the root mean square value of Gaussian distribution and $C_{\gamma_u} = \frac{\sigma_{\gamma_u}}{\sqrt{\pi}}$ is the normalized coefficient.

After the distribution of γ_u has been obtained, the general behaviour of the ensemble-average speed $\overline{\beta}$ dependence on the randomness strength W can be obtained from expression (35). On the other hand, this behaviour can also be obtained by numerically simulating Eq.(1). In the simulation, GS propagates through 4000 lattice sites. Because of the limitation of computational source, 20 configurations are adopted to obtain the ensemble-average speed. The values of ensemble-average speed that depends on the random strength, obtained separately by the two methods, are plotted in Fig.7. From this figure we can see that the ensemble-average speed calculated by the EPP (solid line) coincides with the one obtained by the numerical simulations (dot-dash line). This also proves that the EPP is a good tool for describing the GS propagation in this weak random system. Moreover, from Fig.7, we can see that with the increase of random strength, the ensemble-average speed decreases slowly and the reduction is parabolic.

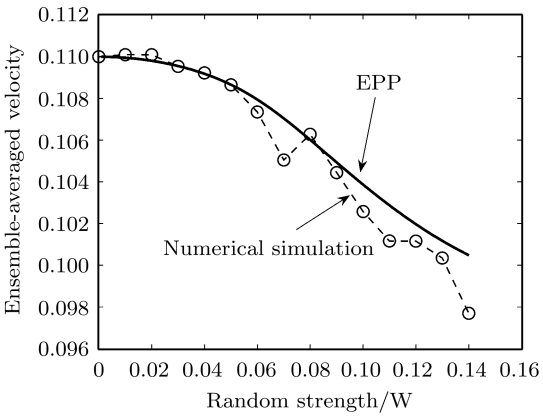


Fig.7. The ensemble-average speed of GS, $\overline{v}$, versus random strength W. The initial parameters of GS are the same as those in Fig.5. In this case, the coefficients σ_{γ_u} and C_{γ_u} in expression (38) are obtained to be $\sigma_{\gamma_u} = 0.051$ and $C_{\gamma_u} = 2.45$. The relation calculated from the EPP assumption is plotted by the solid line, and the relation obtained by numerical simulation is plotted by the dot-dash line. We find that they accord with each other very well.

The slow reduction of the ensemble-average speed can be explained qualitatively from expressions (33) and (34). Because the random strength is very small in our model, the effective potential U_i is mostly smaller than the critical potential. Then we focus our attention only on the case in which the effective potential is smaller than the critical potential. For $U_i < U_{\mathrm{c}}$, the local speed can be expanded into

$$\beta_i = \beta_0 \left[1 - \frac{U_i}{m_{\mathrm{s}}\beta_0^2} - \frac{1}{2}\left(\frac{U_i}{m_{\mathrm{s}}\beta_0^2}\right)^2 - \cdots\right], \tag{39}$$

then the ensemble-average speed can be written as $\overline{\beta} = \beta_0 \Big/ \left[1 + \frac{C_u W}{m_s \beta_0^2}\overline{\gamma_u} + \frac{3}{2}\left(\frac{C_u W}{m_s \beta_0^2}\right)^2 \overline{(\gamma_u)^2}\right]$, in which the value $\overline{\gamma_u}$ is zero, and the value $\overline{\gamma_u^2}$ is a positive constant. Then in the weak randomness limit ($W \ll 1$), the ensemble-average speed can be approximated as

$$\overline{\beta} = \beta_0 \left[1 - \frac{3}{2}\left(\frac{C_u}{m_s \beta_0^2}\right)^2 W^2 \overline{(\gamma_u)^2}\right]. \tag{40}$$

In expression (39), the change of the local speed comes mainly from the first-order term ($\beta_0 U_i/(m_s\beta_0^2)$) which can be close to β_0, while in expression (40) the reduction of the ensemble-average speed is only proportional to the second-order term, which is very small in our model. This means that although the change of the local speed can be large and the reduction of the ensemble-average speed is very small. On the other hand, the reduction of the ensemble-average speed in expression (40) is proportional to W^2, which means the $\overline{v} - W$ line is parabolic. Moreover, the relationship between the ensemble-average speed and the weak nonlinear randomness can be obtained from expression (40). From expression (40), the reduction of the ensemble-average speed is proportional to the value $\Gamma = W^2\overline{\gamma_u^2}$, and from expression (38), the value (Γ) can be written as $\Gamma = (W^2\overline{\gamma^2})/\sigma_{\gamma_u}^2$, in which $W^2\overline{\gamma^2}$ is the variance of the randomness introduced in the nonlinear potentials. Then the reduction of ensemble-average speed is proportional to the variance of the weak randomness. Since the variance is very small in our model, this also confirms that with the increase of the random strength, the ensemble-average speed reduces slowly.

Finally, we obtain the GS reflection probability dependence on the random strength. The conditions of the reflection case can be obtained from expression (32). When $C_u W\gamma_u > m_s\beta_0^2/2$, GS will be reflected. Then the critical value of the random number can be obtained as $\gamma_u^c = m_s\beta_0^2/(2C_u W)$. And since $C_u < 0$, when $\gamma_u > \gamma_u^c$ then GS will be reflected. And the reflection probability is

$$P_r = \int_{-\infty}^{\gamma_u^c} \rho(\gamma_u) \mathrm{d}\gamma_u. \tag{41}$$

The reflection probability dependence on the random strength is shown in Fig.8. From this figure, we can see that with the increase of the random strength the reflection probability becomes larger. In physics, with the increase of the random strength, the fluctuation of random potentials becomes larger. This means that the probability with which the random potential is larger than the critical potential becomes larger. So, the reflection probability becomes larger along with the random strength.

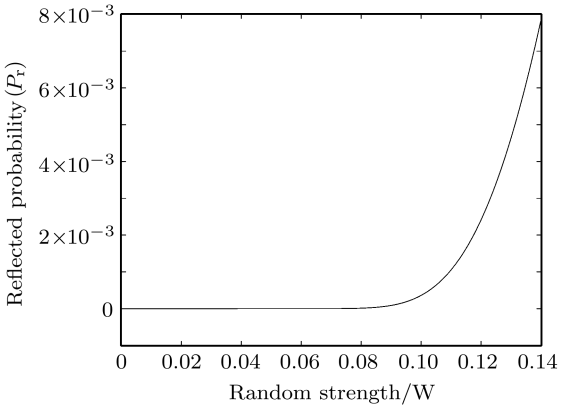


Fig.8. The reflection probability P versus the random strength W. The parameters of GS are the same as those in Fig.5. This figure shows that the reflection probability becomes larger with the increase of W.

5. Summary

The slowly moving matter–wave GS propagation in a weak random nonlinear potential has been investigated in this paper. In this system, the motion of GS can be described by the EPP, in which a GS can be treated as a moving particle. Based on the EPP, the effect of the weak nonlinear randomness on the GS motion is obtained, for example, the GS subjected to a conservative force behaves as a moving particle in random potentials. The detailed interpretation of the force is obtained: the force can be divided into two parts, i.e. the front-part and the back-part, and the force-responses of the randomness in the two parts of GS are different. In addition, the contributions of the randomness to the effective potential are obtained: the contribution due to the local random configuration, and the contributions from GS front-part and back-part that are equal. With the effective potential, the trajectories of GS are well predicted. Finally, the general behaviour that describes the GS motion and the weak spatial nonlinear randomness is found: when the random strength increases, the ensemble-average speed decreases slowly with the decrease of the ensemble-average speed that is proportional to the variance of the randomness and the reflection probability becomes larger. All the results are confirmed by the FDTD simulations based on the GPE.

References

[1] Minguzzia A, Succib S, Toschib F, Tosia M P and Vignolo P 2004 *Phys. Rep.* **395** 223

[2] Morsch O and Oberthaler M 2006 *Rev. Mod. Phys.* **78** 179

[3] Morsch O, Muller J H, Cristiani M, Ciampini D and Arimondo E 2001 *Phys. Rev. Lett.* **87** 140402

[4] Cristiani M, Morsch O, Muller J H, Ciampini D and Arimondo E 2002 *Phys. Rev.* A **65** 063612

[5] Fallani L, Cataliotti F S, Catani J, Fort C, Modugno M, Zawada M and Inguscio M 2005 *Phys. Rev. Lett.* **91** 240405

[6] Greiner M, Mandel O, Esslinger T, Hansch T and Bloch I 2002 *Nature* **415** 6867

[7] Eiermann B, Anker Th, Albiez M, Taglieber M, Treutlein P, Marzlin K P and Oberthaler1 M K 2004 *Phys. Rev. Lett.* **92** 230401

[8] Chen W and Mills D L 1987 *Phys. Rev. Lett.* **58** 160
Chen W and Mills D L 1987 *Phys. Rev.* B **36** 6299

[9] Sterke C M and Sipe J E 1994 *Progress in Optics XXXIII* edited by E. Wolf (Elsevier, Amsterdam)

[10] Sterke C M and Sipe J E 1988 *Phys. Rev.* A **38** 5149
Sterke C M and Sipe J E 1989 *Phys. Rev.* A **39** 5163

[11] Mills D L and Trullinger S E 1987 *Phys. Rev.* B **36** 947

[12] Aceves A B and Wabnitz S 1989 *Phys. Lett.* A **141** 37

[13] Feng J and Kneubühl F K 1993 *IEEE J. Quantum Electron.* **29** 590

[14] Li X and Guo G C 2000 *Chin. Phys.* **9** 1732

[15] Li S M, Wang Q, Wu Z and Wei Q 2001 *Acta. Phys. Sin.* **50** 489 (in Chinese)

[16] Liu N H and Fu J W 2003 *Acta. Phys. Sin.* **52** 1418 (in Chinese)

[17] Liu L H, Tang Z H and Yan J R 2006 *Chin. Phys.* **15** 2638

[18] Louis P J, Ostrovskaya E A and Kivshar Y S 2005 *Phys. Rev.* A **71** 023612

[19] Ostrovskaya E A and Kivshar Y S 2003 *Phys. Rev. Lett.* **90** 160407

[20] Louis P J, Ostrovskaya E A, Savage C M and Kivshar Y S 2003 *Phys. Rev.* A **67** 013602

[21] Efremidis N S and Christodoulides D N 2003 *Phys. Rev.* A **67** 063608

[22] Zobay O, Pötting S, Meystre P and Wright E M 1999 *Phys. Rev.* A **59** 643

[23] Broderick N and Sterke C M 1995 *Phys. Rev.* E **51** 4978
Broderick N and Sterke C M 1998 *Phys. Rev.* E **58** 7941

[24] Fedichev P O, Kagan Yu, Shlyapnikov G V and Walraven J T 1996 *Phys. Rev. Lett.* **77** 2913

[25] Gimperlein H, Wessel S, Schmiedmayer J and Santos L 2005 *Phys. Rev. Lett.* **95** 170401

[26] Aceves A B, Moloney J V and Newell A C 1989 *Phys. Rev.* A **39** 1809

[27] Farrell C and Leonhardt U 2005 *J. Opt.* B: *Quantum Semiclassical Opt.* **7** 1

[28] Brazhnyi V A and Konotop V V 2004 *Mod. Phys. Lett.* B **18** 627

[29] As mentioned above, here x_c is the central position of GS, and for strict GS solutions, it is same to the effective position $x_{\rm eff}$.

[30] For the sites in which $U_i > U_c$, the local v_i speed is set as zero.